Available online at www.sciencedirect.com
SCIENCE DIRECT®
Journal of Nuclear Materials 335 (2004) 410–416
journal of nuclear materials
www.elsevier.com/locate/jnucmat

Laser ablation tests performed on TORE-SUPRA graphite samples

F. Le Guern *, C. Hubert, S. Mousset, E. Gauthier [1], C. Blanc, P. Wodling, J.M. Weulersse

CEA/DEN/DPC/SPC, CEA Saclay, 91191 Gif sur Yvette, France

Received 12 April 2004; accepted 22 July 2004

Abstract

A laser set-up has been implemented in order to evaluate laser detritiation by ablation. First experiments have been performed on TORE-SUPRA samples. A modelling tool has also been developed in order to estimate ablation thresholds. Furthermore, a diagnostic based on Optical Emission Spectroscopy has been implemented and has allowed the real time co-deposited layer removal to follow.

1. Introduction

In D–T fusion reactors, tritium is trapped in a co-deposited layer [1–3] which results from the sputtering of the surface of plasma facing components (C, Be, stainless steel) by plasma during reactor operation. Re-deposition of the sputtered particles together with hydrogen, deuterium and tritium takes place on colder areas inside the reactor. The tritium inventory trapped in this layer could threaten ITER operation [4]. For this purpose, a variety of detritiation processes are under evaluation [5–7]. Ablation by nanosecond laser pulses has been studied as a cleaning process for different applications [8,9] such as grease removal, paint removal and surface nuclear decontamination. We are developing a program in order to study the efficiency of a possible laser-based detritiation process.

A first part of our work has consisted of implementation of a laser set-up to work as well with infra-red (1064 nm), visible (532 nm) and ultra-violet (355 nm) wavelengths and allowing to precisely characterise the laser energy density on the sample. Then, first ablation experiments have been performed. A thermal modelling tool has also been developed. Feasibility tests with instrumentation to allow following in real time the complete removal of the co-deposited layer.

2. Experimental set-up and beam metrology

Precise ablation thresholds and rates measurements can only be performed with a well characterised laser beam. Two main parameters are highly relevant and have been measured: the total energy of the beam incident on the sample surface and the spatial energy distribution at the place of laser-material interaction.

For this purpose, the experimental set-up described below (see Fig. 1) has been implemented. The beam of

* Corresponding author.
[1] Association EURATOM-CEA, CEA/DSM/DRFC, CEA Cadarache, 13108 Saint Paul Lez Durance (France).

0022-3115/$ - see front matter © 2004 Elsevier B.V. All rights reserved.
doi:10.1016/j.jnucmat.2004.07.053

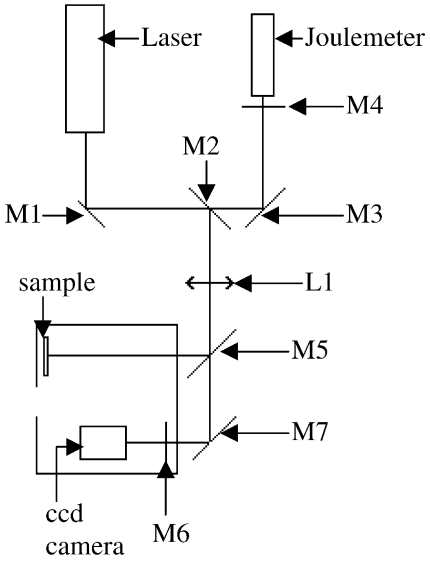

Fig. 1. Experimental set-up.

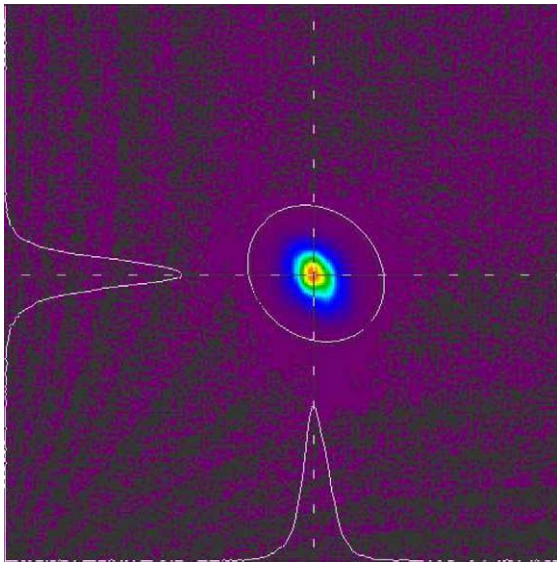

Fig. 2. Laser beam energy distribution on the sample.

a Brilliant laser manufactured by QUANTEL (5 ns pulse duration, 20 Hz repetition rate) reflected by two mirrors (M1 and M2), is focused by a lens (L1) and scanned by a motorised mirror (M5) on the sample.

The beam is characterised by analysing the light transmitted through two mirrors, the first one after the M2 mirror and the second one after the M5 mirror, which are respectively analysed by a joule-meter (to measure the laser beam energy) and a CCD camera (to record the spatial energy distribution of the laser beam) (see Fig. 2).

This experimental set-up can be operated at three wavelengths (1064, 532 and 355 nm). The results presented below have been performed at 532 nm.

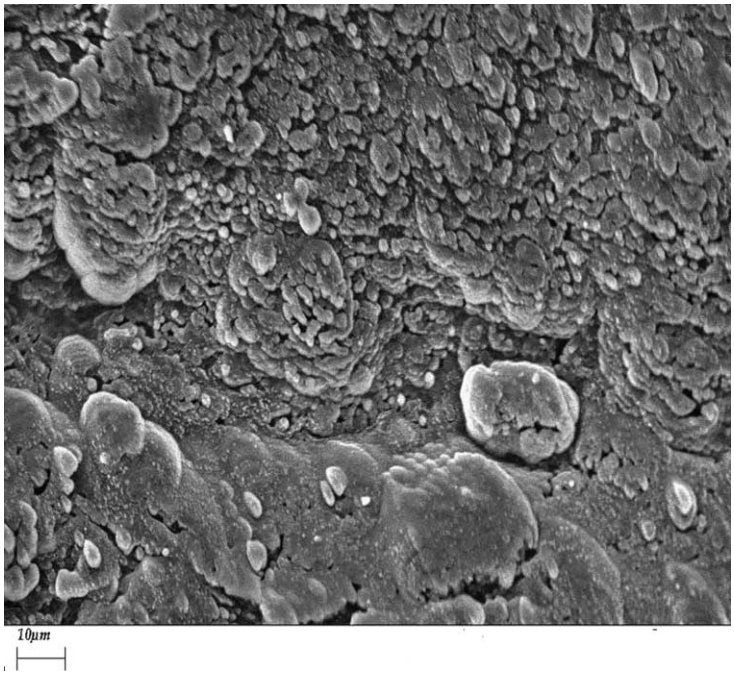

Fig. 3. Image of the co-deposited layer by SEM and bulk.

3. Samples

The graphite (isotropic graphite CL 5890 PL) samples that we tested are from the H-D fusion reactor TORE-SUPRA of CEA in Cadarache, France. They are parts of tiles from the belt limiter that were exposed to 25,000 disharges with ion-temperatures of about 1 keV. The exposure time was of the order of 30 s. The co-deposition layer has been analysed by scanning electron microscopy (see Fig. 3) associated with EDS analysis (see Fig. 4). The co-deposited layer is composed of aggregates. The EDS analyses show that impurities like Fe and Cr are present in this layer, coming from sputtered structural components made of stainless steel. Such impurities have already been described [10] in papers related to co-deposition.

SEM analyses of the tiles have been performed in order to determine the thickness of the co-deposited layer. Fig. 5 presents a cut away in the layer and the bulk performed by Ar ion beam showing an estimated thickness in the range of 20 μm.

4. Ablation results

Ablation efficiency measurements have been done on graphite with and without a co-deposited layer. In both cases, samples have been submitted to 500 shots with variable energy densities. The ablated volumes (craters) have been measured by means of a profilometer. Fig. 6 presents results of ablation. Such curves allow estimation of both the ablation threshold (AT) and the volume ablated per shot.

Two regimes of ablation can be observed:

- a quite linear variation of ablated volume versus energy density up to 9 J cm^{-2};

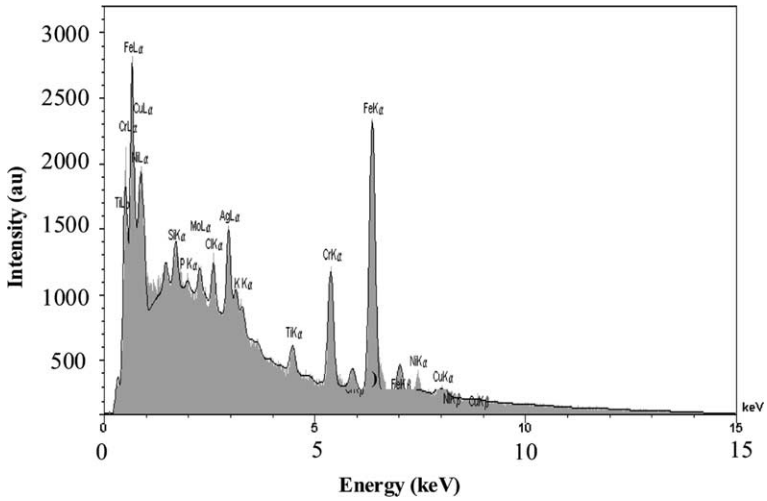

Fig. 4. EDS spectrum of co-deposited layer.

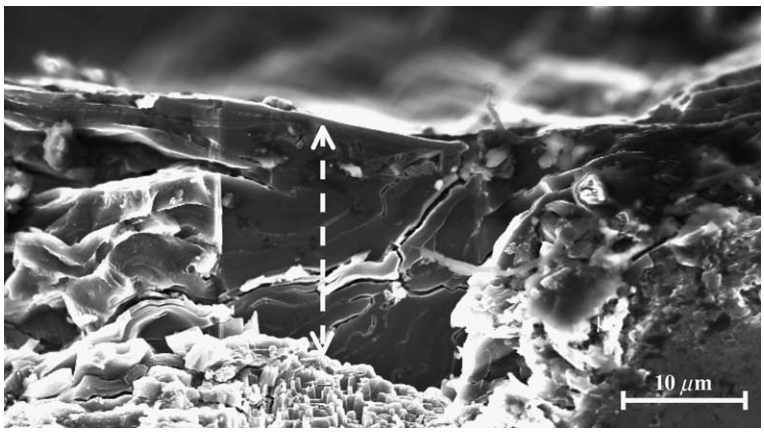

Fig. 5. SEM image after cut away of the co-deposited layer.

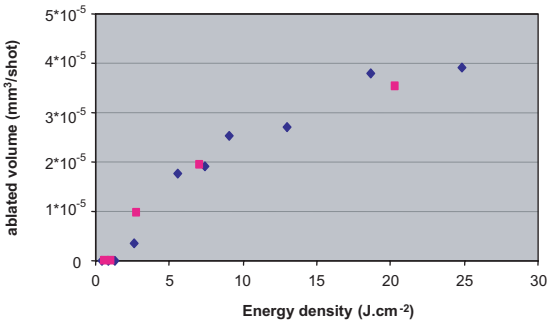

Fig. 6. Ablation measurements on graphite sample (black points) and on graphite sample with a co-deposited layer (pink points). (For interpretation of the references in colour in this figure, the reader is referred to the web version of this article.)

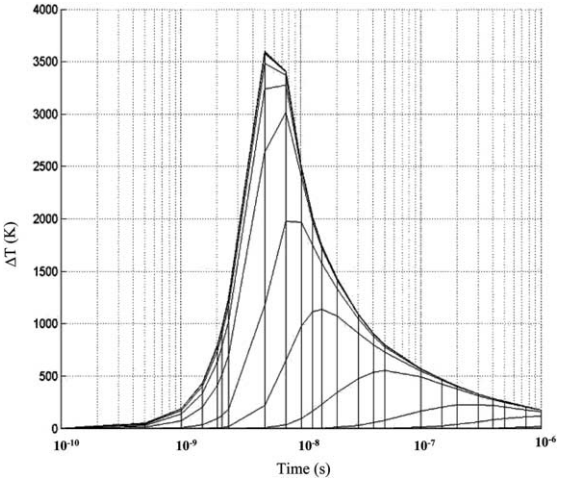

Fig. 7. Temperature depth and time distributions for graphite ($0.7\,cm^{-2}$).

- a very low rise versus increasing energy density beyond $13\,J\,cm^{-2}$.

In order to estimate the ablation threshold of graphite, points corresponding to the first regime have been plotted and a linear regression has been applied. The deduced ablation threshold of graphite is about $1\,J\,cm^{-2}$.

Furthermore, the two regimes identified above can be explained as follows: in the first regime, the interaction occurs between the laser and the surface while in the second case, the plasma (formed by interaction of the laser with ablated atoms) is hotter and its density higher, leading to an absorption of laser energy by the plasma. Then an interaction takes place between the plasma and the surface. This can be demonstrated when looking at the sizes of craters observed in the second case. Indeed, the characteristic diameters at the surface of the crater are much bigger (up to 800 μm) than those of the laser spot (about 300 μm). It appears clearly that for a detritiation process, in order to optimize the efficiency in terms of velocity, the first regime has to be chosen.

When comparing respective ablated volumes at $2.7\,J\,cm^{-2}$ of the graphite sample with co-deposition (see pink point on Fig. 6) and the back of another graphite sample (see black point on Fig. 6), the volume removed in

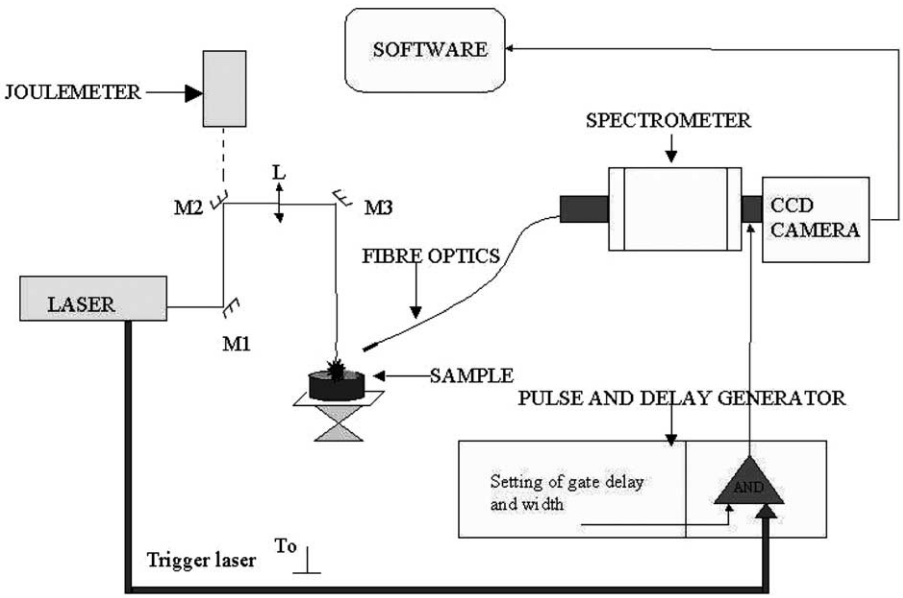

Fig. 8. Optical emission spectroscopy set-up.

the first case seems to be 3 times bigger. This behaviour can be explained by the fact that the co-deposited layer thermal conductivity [7] is lower than for graphite.

5. Thermal model

In order to simplify optimisation and to determine efficient operation parameter ranges of a future laser-based process, we developed, in parallel to the experiments, a laser-matter interaction model. Furthermore, facilities available at DPC/SPAL do not allow for experiments to be performed on beryllium (Be). As a first stage, a simple one-dimensional tool has been developed allowing calculation of the energy deposition in the material and its thermal behaviour, during and after energy deposition taking into account thermal conductivity. The model is based on a numerical resolution of the heat equation [11]. Calculations have been performed (see Fig. 7) in case of graphite taking into account incident laser (532 nm) energy densities of 0.7 and $1\,\mathrm{cm}^{-2}$ respectively. Taking into account the boiling point of graphite (4623 K), it can be deduced from numerical results that its ablation threshold is between 0.7 and $1\,\mathrm{J\,cm}^{-2}$. Such a result is in good agreement with the experimental estimation (see Section 4). Similar calculations, performed for Be, indicate that its ablation threshold is between 0.5 and $0.75\,\mathrm{J\,cm}^{-2}$.

6. Feasability tests performed with an optical emission spectroscopy diagnostic

The Optical Emission Spectroscopy has been quickly identified as a very promising candidate for a process diagnostic:

- It allows, recording lines emitted from the laser induced plasma, to characterize the surface in term of chemical element composition.
- It is a very sensitive technique (low detection threshold <ppm).
- It is convenient to implement (no necessary vacuum, signal collected by optical fibres allowing to let expensive devices outside the contaminated zone).
- It gives information on the surface before and after the treatment by analysing the first and the last pulse. This reduces the number of surface analyses (SEM, Luminescent Discharge Spectroscopy...) needed to be performed before and after laser-matter interaction tests. Post-test analyses are indeed time and cost consumers.
- It is also possible to follow the decontamination by recording in real time specific lines of the contaminated layer or of the substrate.

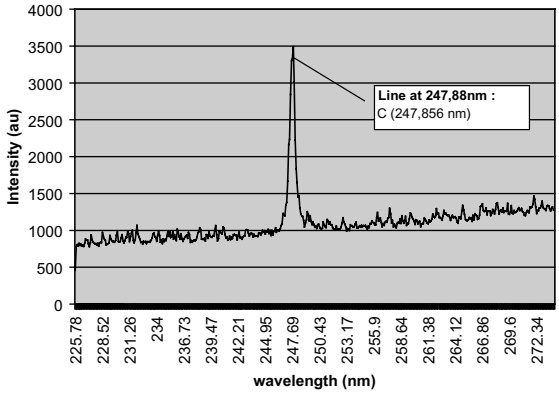

Fig. 9. Optical emission spectroscopy on graphite sample.

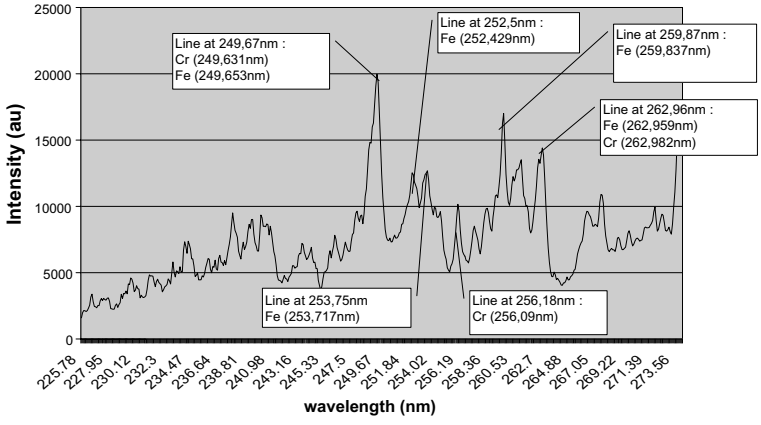

Fig. 10. Optical emission spectroscopy on co-deposited layer.

6.1. Set-up

Fig. 8 represents the experimental set-up which has been implemented on our laser test bench. It comprises four items:

- an optical signal collection system composed of a fibre optic bundle;
- a spectrometer (grating: 1200 lines/mm → resolution: 0.3 nm; spectral dispersion: 40 nm controlled by the mean of a motorised grating from 200 nm up to 800 nm);
- an intensified CCD camera;
- a gate generator.

The gate generator which is directly trigged by the laser monitors the CCD camera acquisition. Two temporal parameters are defined by the operator:

- The delay, after which the CCD starts to record the optical signal, is automatically added to the t0 signal given to the generator by the laser trigger.
- The recording duration (minimum value: 5 ns).

6.2. Spectra recording

A single laser shot has been delivered on a graphite sample (without co-deposition) and the spectrum presented on the Fig. 9 has been obtained. We can identify the strong 247.856 nm carbon line. The same experiment has been repeated on the sample with a co-deposited layer in order to record the co-deposited layer spectrum (see Fig. 10). This one reveals the presence of Fe and Cr which have already been identified by the EDS analysis (see Fig. 4). Nine additional shots have then been done on the same location as the first shot and the plasma emission has been recorded during the plasma created by the last shot. The corresponding spectrum is represented in yellow on the Fig. 11 and is compared to specific spectra of co-deposited layer in violet and graphite in blue. It appears that the specific spectrum of the co-deposited layer has nearly disappeared except a residual line specific of Fe or Cr (the resolution of the device does not allow to discriminate). A post-analysis EDS performed on a graphite sample with co-deposited layer irradiated by laser in similar conditions is shown on the Fig. 12. When comparing

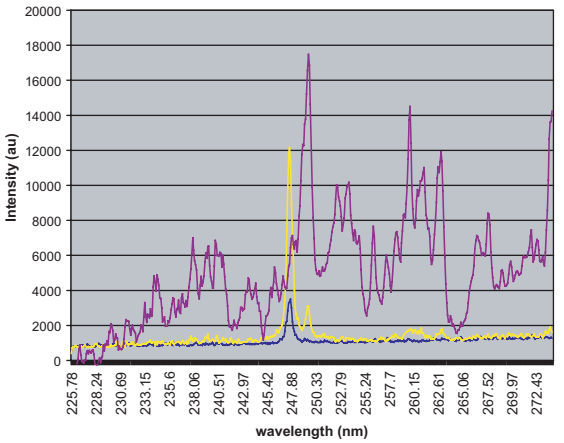

Fig. 11. Optical emission spectroscopy spectra before and after laser treatment. (For interpretation of the references in colour in this figure legend, the reader is referred to the web version of this article.)

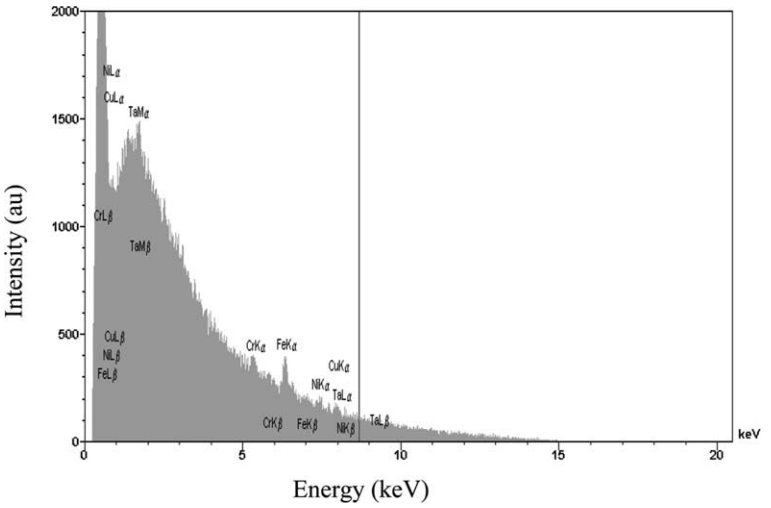

Fig. 12. EDS analysis after laser treatment.

the recorded spectrum with another one realised on the same sample (see Fig. 4) before laser treatment, a decrease of metallic line intensities can be observed, and confirms qualitatively the observations obtained with optical emission spectroscopy. The presence of Fe or Cr is probably due to a diffusion of this impurity deep in the bulk of graphite. The depth of diffusion must be estimated in further studies.

6.3. Future prospects

This technique could also be used as an in-vessel diagnostic allowing to determine co-deposition:

- locations;
- thickness;
- compositions.

7. Conclusion

In this first part of the research work, a laser set-up has been implemented which allow the performance of well controlled ablation experiments with ultra-violet, visible and infra-red wavelengths. Furthermore a protocol to estimate ablation thresholds and rates for variable materials is now available. First ablation measurements have been obtained at 532 nm for TORE-SUPRA samples. It seems that the co-deposited layer is removed at this wavelength more easily than graphite, but this has to be confirmed.

A thermal model has been developed and gives quite good results in terms of ablation threshold prediction.

Finally we have performed feasibility tests with an Optical Emission Spectroscopy device. We have demonstrated that such a method allows the discrimination of the graphite and the co-deposited layer thanks to specific lines of Fe and Cr elements present in the co-deposited layer. This diagnostic will permit both the decrease of the number of analytical tests needed to optimise laser detritiation and to follow in real time co-deposited layer removal (in order to avoid or limit tile de-conditioning). Furthermore it could be used as an in-vessel diagnostic in order to localize co-deposition and determine its composition.

References

[1] R.A. Causey, J. Nucl. Mater. 300 (2002) 91.
[2] Y. Youle, A.A. Haasz, J. Nucl. Mater. 248 (1997) 64.
[3] M. Friedrich, W. Pilz, G. Sun, R. Behrisch, C. Garcia-Rosales, N. Bekris, R.-D. Penzhon, in: Proc. 14th Int. Conf. On Ion Beam Analysis, 26–30 July 1999, Nucl. Instrum. and Meth. B 161–163 (2000) 216.
[4] C. Federici, R. Anderl, J.N. Brooks, R. Causey et al., Fus. Eng. Des. 39&40 (1998) 445.
[5] A.A. Haasz, J.W. Davis, J. Nucl. Mater. 256 (1998) 65.
[6] K. Maruyama, W. Jacob, J. Roth, J. Nucl. Mater. 264 (1999) 56.
[7] C.H. Skinner, C.A. Gentile, A. Carpe et al., J. Nucl. Mater. 301 (2002) 98.
[8] J.R. Costes, A. Briand, B. Remy, P. Mauchien, in: Proceedings of the International Topical Meeting on Nuclear and Hazardous Waste Management Spectrum-96, vol. 3, 1996, p. 1760.
[9] T. Fourrier, G. Schrems, T. Mühlberger, J. Heitz, N. Arnold, D. Baüerle, M. Mosbacher, J. Boneberg, P. Leiderer, Appl. Phys. A 72 (2001) 1.
[10] M. Rubel, P. Wienhold, D. Hildebrandt, J. Nucl. Mater. (2001) 473.
[11] D. Bäuerle, Laser Processing and Chemistry, Springer edition, Berlin, 2000.